JOURNAL OF CATALYSIS 30, 155–168 (1973)

The Coking of Porous Catalysts

Catalytic Dehydration of 2-Methyl-3-buten-2-ol Over Alumina*

G. GRECO, JR., F. ALFANI, AND F. GIOIA†

Istituto di Principi di Ingegneria Chimica, Università di Napoli, Italy

Received August 7, 1972; revised December 4, 1972

The main purpose of the present paper is to discuss the deactivation patterns of catalytic reactions in which the reaction rate is reduced by coke formation on the active catalyst surface. In order to obtain experimental data which could confirm the validity of theoretical predictions, the dehydration of 2-methyl-3-buten-2-ol over alumina has been studied.

Of all the possible mathematical models of the coking phenomenon, only two have been considered which are in agreement with the basic features of the reacting system chosen, i.e., the main reaction is zero order with respect to the reactant, and that poisoning is in series with respect to the main reaction.

Therefore, only preliminary experimental information was needed to formulate the mathematical models. These have shown good agreement with the experimental results, although a more detailed experimental study will be needed to perform a better discrimination among them.

INTRODUCTION

In this paper we discuss the mechanism of catalyst deactivation due to coke deposition on the surface of catalyst pellets.‡ This is a frequently observed phenomenon in many organic reactions taking place at relatively high temperatures over solid catalysts.

Coking can be looked upon as a particular case of the more general problem of catalyst poisoning. The features which single it out from other poisoning situations are (a) coke is usually assumed to form directly on the active surface where it is deposited, and (b) that it is originated by a parasitic reaction which can be either in parallel or in series with the main reaction.

Up to now this phenomenon has been mainly approached following two complementary lines. The first has been devoted to the study of the chemistry of the coking reaction in order to obtain information on its kinetics, on the chemical nature of the coke deposits and their interactions with the active sites of the catalyst—see for example (*1*, *2*). On the other hand, both theoretical and experimental work has had the purpose of linking the overall activity of the porous catalyst to coke deposition, i.e., in determining relationships between the effectiveness factor and the amount of coke deposited.

The first work in which the last problem was expressly treated was that of Wheeler (*3*, *4*). In dealing with the more general problem of poisoning, he showed that, at the steady state, the effect of coke deposition on the effectiveness factor of a porous catalyst is strongly dependent, among other things, on the way the poison distributes inside the pores. The quite different behavior of catalysts in the two limiting

* This work was presented at the 4th International Congress of Chemical Engineering, Chemical Equipment Design and Automation (CHISA), 11–15 September 1972, Prague, Czechoslovakia.

† Present address: Istituto di Chimica Applicata, Università di Cagliari, Italy.

‡ Nomenclature used in this paper is defined in a section on the last page of this paper.

cases he studied, namely uniform poisoning and pore mouth poisoning, is in fact well known. Since then, the aim of many investigators working on this problem has been to overcome the limitations of Wheeler's model, which mainly consist in its being a steady state analysis. In fact, all poisoning processes are essentially unsteady state phenomena.

Therefore, on a more realistic basis, much theoretical work has since aimed at studying the transient behavior of a porous catalyst subject to poisoning and sometimes specifically to coking. Unfortunately, almost all these studies lack experimental data [except (*5, 6*)]. Furthermore, even when the problem of coking is explicitly treated (*7*), the analyses have to be indeed considered as rather dealing with the case in which the deactivating agent is already contained in the reactant mixture. On the contrary, coking is peculiar inasmuch as the poison is produced by a side reaction within the catalyst itself.

Thus, in order to be realistic and applicable to practical cases, a model that proposes to describe coking in a porous catalyst has to take into account mainly the interferences between the poisoning reaction and reactant or product concentration profiles. Furthermore, as the kinetics of the coking reaction are generally not known a priori, it is necessary to screen among various models on the basis of experimental information to identify the one that fits the case under examination. Such a procedure has been adopted in the present study.

Experimental

Reacting System

In order to obtain experimental data which could be of both industrial interest and of easy and straightforward interpretation, the catalytic dehydration of 2-methyl-3-buten-2-ol (MBE) to isoprene over alumina has been chosen. This reaction is the main step in an industrial starting from acetylene, hydrogen and process for the production of isoprene acetone (*8–10*).

This specific coking process is peculiar inasmuch as the kinetics of the reaction are zero-order with respect to MBE within the concentration range explored. This statement derives from previous work on the system and has been confirmed by the authors during preliminary kinetic runs which will be discussed later in the present paper.

The main known features on MBE dehydration are: (i) the reaction is endothermic $\Delta H = 8.800$ cal/gmole), (ii) in industrial practice it takes place at 260–300°C, (iii) the catalyst used is commercial alumina, (iv) the industrial reactor follows an intermittent working path due to regeneration breaks required for restoring the catalyst activity after it has been strongly reduced by coke deposition, and (v) the feed to the reactor is, in the industrial process, pure MBE.

In all the experimental runs which will be discussed, the feed composition has been at the lower end of the immiscibility range between MBE and water, i.e., 14.5% by weight in MBE. The reason for this choice was to minimize temperature gradients within the catalyst pellets and the reactor. The catalyst used was Harshaw Al 0104 commercial alumina in the form of ¼ in. pellets.

Experimental Apparatus (11)

The general layout of the experimental apparatus is shown in Fig. 1. It consists of a feed tank connected with a burette which allows the flow rate to be measured, a volumetric pump, a fixed bed tubular reactor immersed into a molten salt thermostatic bath, a water-cooled condenser and a collecting vessel for the reaction products. The thermal control of the bath has been achieved by means of an on–off controller which ensured temperature excursions of less than ±2°C.

The reactor has been made from a stainless steel tube 32 mm o.d., 30 mm i.d., 210 mm long. It has been filled with stainless steel cylinders of the same dimensions as the catalyst pellets into which the catalyst has been diluted. A layer of stainless steel cylinders without admixed catalyst acted

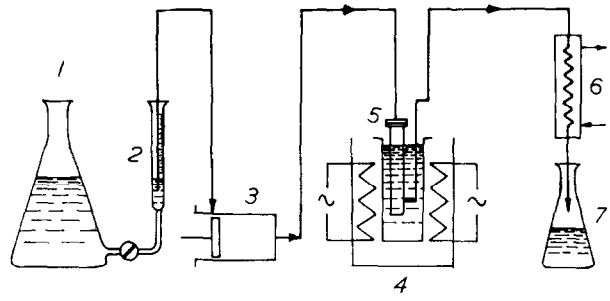

FIG. 1. General layout of the experimental apparatus: (1) feed tank, (2) burette, (3) volumetric feed pump, (4) furnace, (5) reactor, (6) condenser, (7) collecting vessel for reaction products.

as a preheating and vaporizing section for the liquid feed.

The condensed reaction products gave rise to two separate liquid phases, one (the "organic phase") which included all the isoprene formed, a very small amount of the unreacted MBE and traces of organic compounds originated by side reactions, the other (the "aqueous phase") which was mainly formed by water and approximately all the unreacted MBE.

The analyses were performed by periodically sampling fixed amounts of the "aqueous phase" which were blended with a constant volume of ethyl alcohol used as a tracer for the gas-chromatograph analyses. The gas chromatograph was of the flame-ionization detector type, equipped with a 3.50 m long, 3 mm i.d. column, filled with Carbowax 20 m 2% over Chromosorb P60 80 mesh. The carrier flow rate (Nitrogen) was 40 N cc/min and the column temperature 90°C.

Previous calibration runs produced a conversion (moles of MBE reacted/moles of MBE fed) vs (MBE area/ethyl alcohol area) plot, which, upon assumption of negligible MBE content in the organic phase, was used throughout all the experimental runs. This assumption, which gave rise to the technique of analyzing the aqueous phase only, is mainly justifiable because of the small amount of the organic phase relative to the aqueous one and because of the lower MBE solubility in the first. However, in order to minimize error, we waited for a sufficient time to elapse before performing an analysis that, due mainly to isoprene evaporation, a considerable reduction in volume of the organic phase was attained. This in turn implied the transfer of almost all the MBE initially contained in the organic phase to the aqueous one.

RESULTS

Kinetic Runs

In order to verify the correctness of zero-order kinetics for the dehydration reaction, preliminary kinetic tests have been carried out. The results are summarized in Fig. 2, in the form of an x vs Q/w diagram. Standard conditions have been adopted throughout the runs, i.e., (i) constant feed composition (14.5% by weight in MBE); (ii) same catalyst weight (4 g).

No problem arose due to catalyst decay because of the short times needed to complete the kinetic measurements as com-

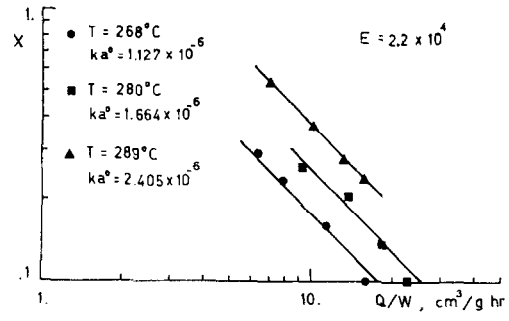

FIG. 2. Results of the kinetic runs (for dimensions, see list of symbols).

pared to the ones implied in an appreciable coking effect, as will be shown later. However, for each temperature explored, a fresh batch of catalyst has been used.

An inspection of Fig. 2 shows how the data fit linear correlations with slope -1, which confirms zero-order kinetics.

In order to ascertain whether the kinetic constants which one could evaluate by means of these data are affected by resistance to mass transfer within the catalyst pellets, at least some order of magnitude evaluations of the effectiveness factor need to be made.

Assuming zero-order kinetics throughout the whole MBE concentration range to hold, i.e.,

$$\begin{aligned} r^0 &= ka^0, \qquad \text{for } c \neq 0, \\ r^0 &= 0, \qquad \text{for } c = 0, \end{aligned} \tag{A}$$

the Thiele modulus is expressed by

$$\Phi = (ka^0R^2/c^0D)^{1/2} \tag{B}$$

It is well known (*12*) that, for a kinetic system such as (A), taking place into a spherical catalyst pellet, a value of $\Phi = \sqrt{6}$ implies $\gamma = 0$ at $\zeta = 0$; values of $\Phi < \sqrt{6}$ mean that γ never reaches a zero value within the pellet whilst, for $\Phi > \sqrt{6}$, $\gamma = 0$ at some value λ° of the dimensionless radius which can be determined once the value of Φ is known. This calculation can be performed making use of the relationship

$$\lambda^{\circ 3} - 1.5\lambda^{\circ 2} - (3/\Phi^2 - 0.5) = 0.$$

Due to the zero-order kinetics, $\Phi \leq \sqrt{6}$, therefore, implies a value of unity for the effectiveness factor η; $\Phi > \sqrt{6}$ determines situations in which η is less than unity and can be expressed as the ratio between the volume of the spherical shell of radii λ° and 1, and the volume of the whole catalyst sphere of unity dimensionless radius.

TABLE 1
RESULTS OF POROSIMETRIC TESTS AND CALCULATED VALUES OF THE DIFFUSION COEFFICIENTS

ϵ	$\bar{r}_i$	$\bar{r}_a$	ϵ_i	ϵ_a
0.743	60	1.5×10^4	0.496	0.247
T°	D_{12}[*19*]	D_k	D	
345	0.366	0.0156	0.0328	
271	0.284	0.0146	0.0257	

The pore-size distribution of the catalyst pellets having been previously determined through porosimetric tests, an estimate has been performed of the diffusivities of MBE at the various experimental temperatures making use of the "parallel bundles of pores" model (*13–15*) on the assumption of a tortuosity factor of three and taking into account the catalyst void fraction (see Table 1).

It can be seen that, under the experimental conditions adopted, neither external nor internal mass and heat transfer resistances affected the process. The calculations (see Tables 2 and 3) have been performed for more drastic temperature and conversion conditions than those relative to the kinetic runs (see Figs. 3 and 4).

The statement of negligible internal and external resistances holds within the limits of confidence which can be ascribed to calculated values of transfer coefficients and diffusivities. However, because of the effectiveness factors being practically constant within all the runs carried out at each temperature, the fit of the kinetic data to a -1 slope straight line in any case confirms zero order kinetics.

The values of the kinetic constants, determined on the basis of experimental data

TABLE 2
EVALUATION OF EXTERNAL HEAT AND MASS TRANSFER RESISTANCES (*20*)

T°	C°	h	k_c	q	N	$C^\circ - C_s$	$T^\circ - T_s$
345	9.25×10^{-7}	1.45×10^{-3}	4.17	3.6×10^{-3}	4.1×10^{-7}	9.85×10^{-8}	2.45
271	1.05×10^{-6}	1.51×10^{-3}	4.66	8.0×10^{-4}	9.1×10^{-8}	1.95×10^{-7}	0.53

TABLE 3
EVALUATION OF INTERNAL HEAT AND MASS TRANSFER RESISTANCES (*21*, *22*)

T	β	E/RT	Φ	η
345	-8.67×10^{-4}	18.0	3.43	0.88
271	-8.75×10^{-4}	20.4	1.83	1.00

at three different temperatures, together with the resulting activation energy, have been reported in Fig. 2.

Poisoning Runs

The results of the poisoning runs are reported in Figs. 3 and 4. On the left side, ordinate axis values of x (conversion) are reported; on the right side ordinate axis a dimensionless variable ξ appears which is defined as the ratio between present and initial reaction rate. The abscissa is reaction time measured in hours starting from the beginning of the poisoning test.

Two separate runs have been performed, whose experimental conditions are reported in Figs. 3 and 4.

Upon inspection of these diagrams, it can be seen that in both cases no appreciable catalyst decay takes place during at least the first ten hours of the test. This enabled the kinetic runs to be performed with no prejudice resulting from catalyst deactivation. In the course of preliminary poisoning tests, some amount of reversibility in coke deposition has been observed which made itself apparent since, after over-night interruptions of the feed

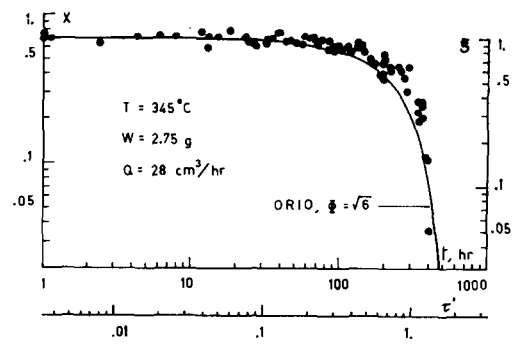

FIG. 3. Results of the poisoning runs, T = 345°C.

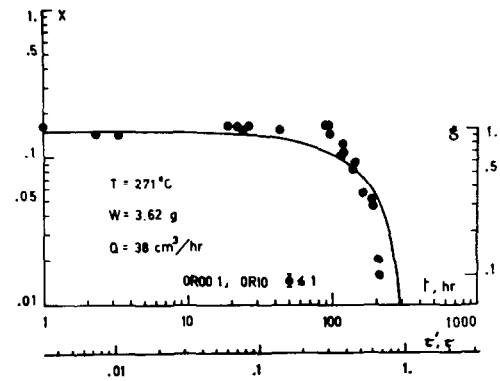

FIG. 4. Results of the poisoning runs, T = 271°C.

flow rate, the catalyst at least partially recovered its activity (*1*).

The main conclusion which can be drawn from the experimental results is that a total catalyst deactivation is achieved within a finite poisoning time.

Direct inspection of catalyst particles taken out from the reactor at an intermediate poisoning time has shown, see Fig. 5, that the outer shells of the catalyst pellets were more markedly "coked" than the inner ones, thus indicating that coking rate is a maximum at the outer surface and decreases with decreasing radial distance. This is true for reaction temperatures of 350°C and is not the case for temperatures in the range 270–290°C.

MATHEMATICAL MODELS

On the basis of the experimental evidence discussed above, the main features of the mathematical models for the poisoning process should be: (i) the main reaction is zero order with respect to the reactant; (ii) the rate of the main reaction is an increasing function of the amount of available active sites; (iii) the coke formation is parallel with and not consecutive to the main reaction. In other words the reactant (MBE) itself directly contributes to the poisoning which is not product (isoprene) dependent; (iv) the poisoning reaction is either homogeneous or, if catalytic, is not dependent on the same active sites as the main reaction.

That the main reaction is of zero-order kinetics has clearly been shown in the

kinetic runs section; on the other hand, statements (ii), (iii) and (iv) need further illustration.

That the rate of the main reaction depends as (ii) upon the availability of some active surface, which is affected by coke formation, is clearly shown by the catalyst deactivation itself. As already outlined in the previous paragraph, the coking rate attains a maximum at the outer catalyst surface, where the reactant (MBE) concentration is at a maximum value also. Viceversa, the corresponding product (isoprene) profile exhibits decreasing concentration values for increasing distances from the center of the catalyst pellet. Unless an unlikely negative order of reaction is appealed to, this implies that the poisoning reaction is reactant (MBE) dependent.

Statement (iii) stems from the complete deactivation time being finite. As a matter of fact, if the coke production took place on the same active sites as the main reaction, its rate should be decreasing with decreasing catalyst activity. This, in turn, should imply catalyst deactivation to be an asymptotic process towards zero activity in an infinite reaction time. This not being the case, the conclusion has to be reached that either the poisoning reaction is homogeneous or it requires active sites which are different in nature from the ones involved in the main reaction and not affected by coke formation. In any case, as already mentioned, the coke, once formed, has to affect the catalyst surface which is active towards the main reaction either by chemisorbing on it or by shielding it in such a way as to prevent the reactant to reach it.

Following all the above considerations, two different models have been considered. In both, the main reaction has been supposed to be zero order in MBE and, for the sake of easiness, first order in active surface, while the poisoning reaction has been assumed to be MBE-dependent and zero order in active surface.

The first model—0R00—(main reaction 0 order kinetics, Reactant (R) is coke producing, coking is 0 order with respect to reactant, coking is 0 order with respect to active surface) assumes coking kinetics to be zero order in MBE too; the second—0RI0—(main reaction 0 order kinetics, Reactant (R) is coke producing, coking is I st order with respect to reactant, coking

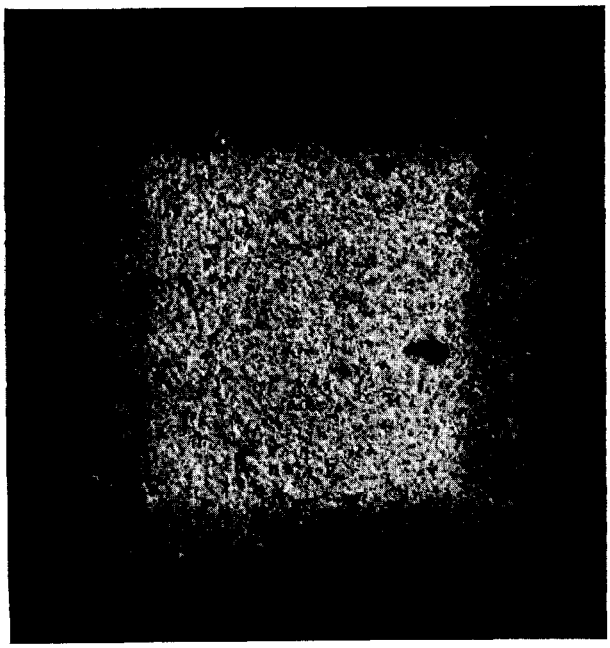

Fig. 5. Partially deactivated catalyst pellet, T $\simeq$ 350 °C.

is 0 order with respect to active surface), on the other hand, considers the coking reaction rate to be first order in MBE.

Two different cases have been taken into account for each model: case 1, in which the initial effectiveness factor for the main reaction is one, and case 2, in which an η value of less than one occurs. In summary, four different models arose which in the following will be referred to as: 0R001, 0R002, 0RI01, and 0RI02, respectively.

Before describing into further detail the above models, the general mathematical assumptions which have been made in the course of their treatment need to be discussed and justified on the basis of physical arguments.

It has been considered that: (i) in the reactant mass balance differential equation the gas-phase accumulation term need not to be taken into account; (ii) in the reactant mass balance the consumption term due to coke production could be neglected; (iii) reactant concentration at the outer surface of catalyst pellet was constant with time and within the whole reactor; (iv) although the catalyst used was in form of cylindrical pellets, the mathematics have been developed on the basis of a spherical geometry. This has been done in order to simplify the mathematical treatment; however, the results are applicable to different geometries (*16*) upon definition of a suitable characteristic dimension. (v) external mass and heat transfer resistances could be neglected.

Assumption (i) is justified through the comparison between the time scales of catalyst deactivation and reset of gas phase reactant concentration profiles inside the pellet. Accordingly, the reaction has been assumed to be, at every time considered, in the steady state situation pertaining to the particular available surface distribution; see also (*17*).

Assumption (ii) derives from the coke formation being very much slower than the main reaction so that the amount of reactant involved in coke production is negligible as compared to that converted to product. If this was not the case, catalyst deactivation would have been a much faster process, due to the relatively small amount of "coke molecules" needed to completely cover the available internal area of the catalyst.

Assumption (iii), whose usefulness in mathematical manipulation is obvious, is realistic as far as the reactor gives rise to a differential conversion. This is the case mainly for the experimental run described in Fig. 4.

A last assumption had been implicitly made throughout the treatment of all the models considered, i.e., coke deposition does not affect reactant diffusion. In other words no reduction in pore size has been assumed to take place in the course of the whole process.

The increase in catalyst weight due to coke formation was found to be 14.5% at the end of the poisoning run at 345°C.

0R001 Model (11)

The reactant mass balance equation is, in dimensionless form,

$$\frac{d^2\gamma}{d\zeta^2} + \frac{2}{\zeta}\frac{d\gamma}{d\zeta} = \Phi^2\alpha, \tag{1}$$

with B.C.'s.

$$\zeta = 1, \qquad \gamma = 1,$$
$$\zeta = 0, \qquad d\gamma/d\zeta = 0.$$

The available area balance is expressed by

$$d\alpha/d\tau = -1 \tag{2}$$

with I.C.

$$\tau = 0, \qquad \alpha = 1.$$

Integration of Eq. (1) gives

$$\gamma = 1 - (\Phi^2\alpha/6)(1 - \zeta^2) \tag{3}$$

while Eq. (2) in integrated form produces

$$\alpha = 1 - \tau. \tag{4}$$

Substitution of Eq. (4) into Eq. (3) differentiation with respect to ζ and setting $\zeta = 1$ eventually gives:

$$d\gamma/d\zeta|_{\zeta=1} = \Phi^2(1 - \tau)/3 \tag{5}$$

For $\tau = 0$, the corresponding value being:

$$d\gamma/d\zeta|_{\zeta=1,\tau=0} = \Phi^2/3,$$

one gets:

$$\xi = 1 - \tau, \qquad (6)$$

which, as all the previous equations, is valid for

$$0 \leq \tau \leq 1.$$

In Fig. 6, a plot of ξ vs τ as calculated through Eq. (6) is reported.

Model 0R001 leads to the typical "uniform coking" case and is the only one which can be handled formally since it does not need numerical integration procedures.

0R002 Model (11)

The reactant mass balance differential equations which, in this case, describe the phenomenon are, moving from the outside of the catalyst pellet toward its center:

$$\frac{d^2\gamma}{d\zeta^2} + \frac{2}{\zeta}\frac{d\gamma}{d\zeta} = 0 \qquad \text{(pure diffusion)} \quad (7)$$

with B.C.'s.

$$\zeta = 1, \qquad \gamma = 1,$$
$$\zeta = \pi(\tau), \qquad \gamma[\pi(\tau)_+] = \gamma[\pi(\tau)_-],$$

$$\frac{d^2\gamma}{d\zeta^2} + \frac{2}{\zeta}\frac{d\gamma}{d\zeta} = \Phi^2\alpha \qquad \text{(diffusion and reaction)} \quad (8)$$

with B.C.'s.

$$\zeta = \pi(\tau) \qquad \gamma[\pi(\tau)_-] = \gamma[\pi(\tau)_+]$$
$$\zeta = \lambda(\tau) \qquad \frac{d\gamma}{d\zeta} = 0$$

and

$$\gamma = 0 \qquad \text{(absence of reactant)} \quad (9)$$

for

$$0 \leq \zeta \leq \lambda(\tau).$$

In order to achieve a better understanding of Eqs. (7–9) together with the corresponding B.C.'s and before dealing with the available area balance equations, a short illustration of the physical phenomenon needs to be made.

At $\tau = 0$, depending upon the value of Φ, γ reaches a zero value for, say, $\zeta = \lambda^\circ$. Therefore, at $\tau = 0$, the catalyst pellet can be divided into two different regions: the first ranging from $\zeta = 0$ to $\zeta = \lambda^\circ$ in which, γ being equal to zero, neither reaction nor poisoning occur and the second, bounded by $\zeta = \lambda^\circ$ and $\zeta = 1$, in which both reaction and coking take place. For $0 \leq \tau \leq 1$, due to catalyst deactivation the value of ζ[say λ (τ)] at which $\gamma = 0$, moves progressively towards the center of the pellet.

At $\tau = 1$, the area which was initially available in the region between $\zeta = \lambda^\circ$ and $\zeta = 1$ is completely and simultaneously "coked." For $\tau = 1$, therefore, a moving boundary of complete deactivation say π (τ) starts penetrating the catalyst pellet from the initial value $\pi(1) = \lambda^\circ$.

In summary, starting from $\tau = 1$ onwards, the catalyst pellet can be divided into three different regions: (a) $0 \leq \zeta \leq \lambda(\tau)$, which has not yet been reached by the reactant; (b) $\lambda(\tau) \leq \zeta \leq \pi(\tau)$, where both reaction and coke formation occur; (c) $\pi(\tau) \leq \zeta \leq 1$, where the deactivation

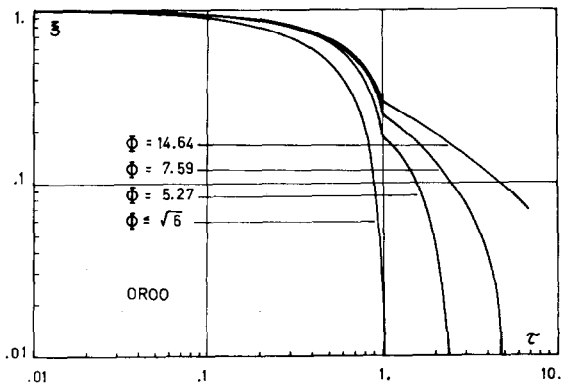

FIG. 6. Theoretical results for 0R00 model.

is total and a pure diffusion mechanism takes place for both reactant and product.

Depending upon the value of Φ, $\lambda(\tau)$ could reach the value $\zeta = 0$ for $\tau < 1$; in this case region (a) disappears before $\pi(\tau)$ starts its movement. In any case, for some value of τ, which again depends upon Φ, $\lambda(\tau)$ attains a zero value. From this time onwards the reactant concentration at the center of the pellet steadily increases from $\gamma = 0$ up to $\gamma = 1$. The last value is reached when also $\pi(\tau) = 0$, i.e., when the whole pellet is completely deactivated and, therefore, the concentration inside it is everywhere equal to unity.

In the light of the above considerations, the available area balance (for a given value of Φ) is:

$$\begin{aligned} &\text{for } \lambda^\circ \leq \zeta \leq 1, && \alpha(\tau) = 1 - \tau, && \text{for } \tau \leq 1, \\ &&& \alpha(\tau) = 0, && \text{for } \tau > 1, \end{aligned} \tag{9a}$$

$$\begin{aligned} &\text{for } 0 \leq \zeta \leq \lambda^\circ, && \alpha(\tau, \zeta) = 1, && \text{for } \tau \leq \tau^*(\zeta), \\ &&& \alpha(\tau, \zeta) = 1 - \tau + \tau^*(\zeta), && \text{for } \tau^*(\zeta) \leq \tau \leq [1 + \tau^*(\zeta)], \\ &&& \alpha(\tau, \zeta) = 0, && \text{for } \tau > [1 + \tau^*(\zeta)], \end{aligned} \tag{9b}$$

where $\tau^*(\zeta)$, which is a function of radial position, is the dimensionless time for $\lambda(\tau)$ to attain the given value of ζ.

In Fig. 6 the results of the numerical integration of Eqs. (7–9) are reported in the usual form of a ξ vs τ diagram for various values of Φ.

The values of the Thiele moduli adopted together with the corresponding values of λ° have been reported in Table 4.

It is worthwhile to point out that, on assumption of exactly the same kinetic hypotheses for both the main and the poisoning reaction, results have been obtained, with 0R001 and 0R002 models, which range from the usual "uniform poisoning" model to a situation which is strictly resembling to a "pore mouth" coking, depending only upon the value of the effectiveness factor of the main reaction.

TABLE 4
VALUES OF THE INITIAL REACTANT PENETRATION λ° VS THIELE MODULUS Φ

Φ	λ°
1	0
2.43	0
3.04	0.4
4.13	0.6
5.27	0.7
7.59	0.8

The differential equations reported in the present paragraph, together with the ones pertaining to the following models, have been solved numerically by means of a Runge–Kutta finite differences procedure; details on the programs are reported in (*11*).

ORI01 Model (11)

In this case the dimensionless reactant mass balance equations are given by

$$\frac{d^2\gamma}{d\zeta^2} + \frac{2}{\zeta}\frac{d\gamma}{d\zeta} = 0 \qquad \text{(pure diffusion)} \tag{10}$$

with B.C.'s.

$$\zeta = 1, \qquad \gamma = 1,$$
$$\zeta = \pi(\tau') \qquad \gamma[\pi(\tau')_+] = \gamma[\pi(\tau')_-]$$

and

$$\frac{d^2\gamma}{d\zeta^2} + \frac{2}{\zeta}\frac{d\gamma}{d\zeta} = \Phi^2\alpha \qquad \text{(diffusion and reaction)} \tag{11}$$

with B.C.'s.

$$\zeta = \pi(\tau'), \qquad \gamma[\pi(\tau')_-] = \gamma[\pi(\tau')_+],$$
$$\zeta = 0, \qquad d\gamma/d\zeta = 0.$$

The available area balance gives

$$d\alpha/d\tau' = -\gamma \tag{12}$$

with I.C.

$$\tau' = 0, \qquad \alpha = 1,$$

or, in integrated form,

$$\alpha(\zeta, \tau') = 1 - \int_0^{\tau'} \gamma(\zeta, \tau')d\tau' \tag{13}$$

which holds up to a value of τ' (say $\tau'^*(\zeta)$) such that

$$\int_0^{\tau'^*(\zeta)} \gamma(\zeta, \tau')d\tau' = 1,$$

from $\tau'^*(\zeta)$ onwards:

$$\alpha(\zeta, \tau') = 0$$

A brief physical illustration of the phenomenon is needed for this model too.

Since $\tau' = 0$, the reactant is present in the whole pellet and the main reaction takes place together with poisoning. Due to the first-order coking kinetics assumed, poisoning rate is a maximum at $\zeta = 1$ and a minimum at $\zeta = 0$.

Equation (13) shows how, at $\zeta = 1$, for $\tau' = 1$, $\alpha(1, 1) = 0$. Therefore, at $\tau' = 1$, a moving boundary—$\pi(\tau')$—of completely deactivated area starts penetrating the pellet from the initial value $\pi(1) = 1$. Time $\tau'^*(\zeta)$ is identified by $\pi(\tau')$ achieving the given value of ζ.

A complete catalyst deactivation is attained when $\pi(\tau')$ reaches its final zero value. The results of the numerical integration of Eq. (10) together with Eq. (13) are summarized in Fig. 7.

0RI02 Model (11)

Reactant mass balance equations are

$$\frac{d^2\gamma}{d\zeta^2} + \frac{2}{\zeta}\frac{d\gamma}{d\zeta} = 0 \qquad \text{(pure diffusion)}, \quad (14)$$

with B.C.'s.

$$\zeta = 1, \qquad \gamma = 1,$$
$$\zeta = \pi(\tau'), \qquad \gamma[\pi(\tau')_+] = \gamma[\pi(\tau')_-],$$

$$\frac{d^2\gamma}{d\zeta^2} + \frac{2}{\zeta}\frac{d\gamma}{d\zeta} = \Phi^2\alpha \quad \text{(diffusion and reaction)}, \quad (15)$$

with B.C.'s.

$$\zeta = \pi(\tau'), \qquad \gamma[\pi(\tau')_-] = \gamma[\pi(\tau')_+],$$
$$\zeta = \lambda(\tau'), \qquad \frac{d\gamma}{d\zeta} = 0,$$

and

$$\gamma = 0 \qquad \text{(absence of reactant)}, \quad (16)$$

for

$$0 \leq \zeta \leq \lambda(\tau').$$

The corresponding equation for available area is:

$$\alpha(\zeta, \tau') = 1 - \int_0^{\tau'} \gamma(\zeta, \tau')d\tau', \qquad \tau' \leq \tau'^*(\zeta), \quad (17)$$

$$\alpha(\zeta, \tau') = 0, \qquad \tau' > \tau'^*(\zeta), \quad (18)$$

τ'^* having the same physical meaning as in the previous case.

The main features of 0RI02 model strictly resemble those of 0R002, the major difference being that $\pi(\tau'^*)$ starts its movement from an initial value $\pi(1) = 1$ whilst $\pi(\tau^*)$ started from $\pi(1) = \lambda°$.

In Fig. 7 the results of the numerical integration of Eqs. (14–18) have been summarized.

It should be noted that both 0RI01 and

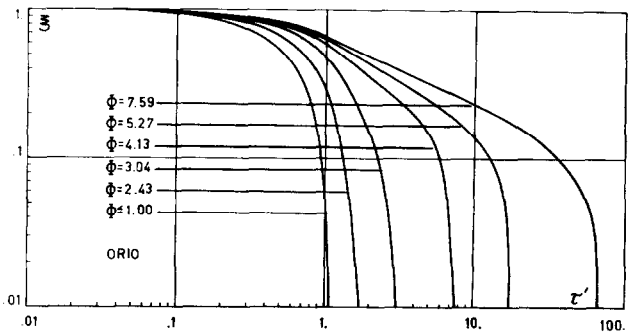

FIG. 7. Theoretical results for 0RI0 model.

0RI02 models are in their nature, typical "pore mouth" poisoning processes.

Discussion

Discussion of Theoretical Results

Figure 6 shows an abrupt variation in slope of ξ vs τ at $\tau = 1$ for 0R002 models, whatever Φ is.

This can be justified on the basis of the definition of ξ and the peculiar characteristics of the model.

The dimensionless overall rate of the main reaction at $\tau = 0$ is given by

$$\rho(0) = \int_{\lambda^0}^{1} 4\pi\Phi^2\zeta^2 d\zeta = (4\pi\Phi^2/3)(1 - \lambda^{03}) \quad (19)$$

at $\tau < 1$, the reactant penetration having achieved the value $\lambda(\tau)$, the dimensionless overall main reaction rate is, recalling Eqs. (9a and 9b),

$$\rho(\tau) = \int_{\lambda(\tau)}^{\lambda^0} 4\pi\Phi^2\alpha(\zeta, \tau)\zeta^2 d\zeta + \int_{\lambda^0}^{1} 4\pi\Phi^2\alpha(\tau)\zeta^2 d\zeta. \quad (20)$$

Hence, for $\tau \leq 1$,

$$\xi = \rho(\tau)/\rho(0) = 3/(1 - \lambda^{03}) \left[\int_{\lambda(\tau)}^{\lambda^0} \alpha(\zeta, \tau)\zeta^2 d\zeta + \int_{\lambda^0}^{1} \alpha(\tau)\zeta^2 d\zeta\right] \quad (21)$$

Deriving Eq. (21) by τ and setting $\tau = 1_-$ one obtains

$$d\xi/d\tau|_{\tau=1_-} = -[1 - \lambda^3(1_-)]/[1 - \lambda^{03}].$$

Recalling Eqs. (9a and 9b), at $\tau = 1_+$, one obtains

$$d\alpha(\tau)/d\tau = 0$$

and

$$d\alpha(\tau, \zeta)/d\tau = -1,$$

therefore,

$$d\xi/d\tau|_{\tau=1_+} = -[\lambda^{03} - \lambda^3(1_+)]/[1 - \lambda^{03}]$$

Inspection of Fig. 7 shows that, for the 0RI01 model, only one curve has been reported at $\Phi \leq 1$. At $\tau' = 0$, the reactant concentration at the center of the pellet, is given by

$$\gamma(0, 0) = 1 - (\Phi^2/6).$$

Therefore, for $\Phi = 1$, $\gamma(0,0) = 0.834$ and hence the reactant concentration throughout the whole pellet is nearly constant. This statement holds even more so for $\tau' > 0$ and $\Phi < 1$. This implies that, for $\Phi \leq 1$, a practically uniform poisoning situation is achieved. Therefore, the definition of the dimensionless time apart, the ξ vs τ or τ' curves for 0R001 and 0RI01 ($\Phi \leq 1$) have to coincide as it is the case.

It should again be noted that, depending upon reactant concentration profiles only, a system which, in its nature, should give rise to a "pore-mouth coking" turns out to be classifiable into a "uniform coking" type.

Comparison between Experimental Results and Theoretical Predictions

Inspection of an arithmetic x vs t plot of the experimental poisoning data at 271°C shows a good linear fit, thus clearly suggesting either an 0R001 or an 0RI01 $\Phi \leq 1$ model. The parameters of the best-fitting straight line have been determined through a linear regression procedure. This enabled the analytical determination of the initial conversion x^0 and of the time t^* at which $x = 0$. In order to convert the diagram x vs t into its standard form ξ vs dimensionless time, it has been necessary to divide the value of x by x^0 and the values of t by t^*. The result is reported in Fig. 4.

The value of t^* is equal to either $a^0/k_2 c^0$ or to a^0/k_1, depending upon the choice among 0RI01 ($\Phi \leq 1$) or 0R001, respectively.

The 0RI01 ($\Phi \leq 1$) model leads to a k_2/a^0 value of 0.85 cm³/gmole sec, whilst the 0R001 model suggests a value of 8.9×10^{-7} sec^{-1} for k_1/a^0. At this stage neither the model nor the value of Φ at 271°C can be determined.

The poisoning data at 345°C show that a linear relationship between x and t does not hold. A four-parameter cubic correlation in the form

$$x = x^0 + a_1 t + a_2 t^2 + a_3 t^3$$

has therefore been adopted and the coefficients x^0, a_1, a_2, a_3 have been determined

by a least squares procedure. The x vs t curve thus obtained has been converted into the form ($\xi = x/x^0$) vs t (hr). A comparison between this diagram and the theoretical curves shows a good fit with both the 0RI02 model, $\Phi = 2.5$ (as shown in Fig. 3), and the 0R002 model ($\Phi = 3.04$). These values of Φ are both in fairly good agreement with the calculated one (see Table 3).

Surprisingly enough, this again implies either: $k_2/a^0 = 0.85$ cm³/gmole sec, or: $k_1/a^0 = 8.9 \times 10^{-7}$ sec^{-1}, respectively.

On the basis of the experimental evidence, as already discussed in the poisoning runs section, at 271°C, η should be equal to unity (i.e., $\Phi \leq \sqrt{6}$) whilst at 345°C, η should be less than unity (i.e., $\Phi > \sqrt{6}$). This statement derives from the order of magnitude evaluations of Φ and also from the catalyst being almost uniformly "coked" at the first temperature and from its showing a more markedly "coked" external layer at 345°C (see Fig. 5). Both the possible model choices are in agreement with these results.

On the other hand, the data at 345°C, depending upon the choice of 0RI02 or 0R002, indicate $\Phi = 2.5$ or $\Phi = 3.04$, respectively. By making use of this result and of the activation energy previously evaluated (see Fig. 2), one gets $\Phi = 0.74$ and $\Phi = 0.90$, respectively, for a temperature of 271°C. Again the agreement with the calculated value is fairly good (see Table 3).

This is still not conclusive as to the determination of 0RI0 or 0R00. In fact, in the first instance, for the experimental system to be an 0RI0 case, at 271°C, Φ should be less than unity, which it is, whilst 0R00 implies Φ at 271°C to be less than $\sqrt{6}$, which is again the case.

The only possible way of discriminating between 0RI0 and 0R00 could be that, for $\Phi = 3.04$, λ^0 is equal to 0.4, i.e., the markedly coked external layer should range from the outer surface to more than half the radius of the pellet, within the limits of the approximation of cylindrical geometry to spherical one. This is clearly not the case, as confirmed by Fig. 5.

On the other hand, the 0RI0 model, whatever $\Phi > \sqrt{6}$, implies a moving boundary of completely deactivated area which starts from the outer surface of the pellet and, for some intermediate value of time, reaches the radial position which can be determined from Fig. 5.

As to the coincidence between the values of either k_2/a^0 or k_1/a^0 at 271 and 345°C, this should imply a negligible activation energy for the coking reaction. However, it should be mentioned that the data at 345°C have been obtained with an integral reactor, i.e., with a reactant concentration which varied along the axis of the reactor from the initial value c^0 to approximately 0.3 c^0. While a complete analysis of the system implies a rather cumbersome mathematical manipulation, it can be roughly assumed that a mean reactant concentration equal to 0.65 c^0 held throughout the whole reactor, on assumption of a CSTR approximation for the plug flow reactor.

On this basis, at 345°C one can determine, for the 0RI02 model

$$k_2/a^0 = 1.31 \text{ cm}^3/\text{gmole sec.}$$

This leads to an activation energy of 3.49×10^3 cal/mole for the coking reaction. In the literature (*18*) some indications are reported which confirm this order of magnitude.

Conclusions

The whole treatment shows how the usual classification of coking processes into "pore mouth" and "uniform" poisoning is somewhat arbitrary and summary.

Indeed, it has been pointed out that, under exactly the same general hypotheses, and depending only upon the value of the Thiele modulus of the main reaction, coking situations can be obtained which show either "pore mouth" or "uniform" poisoning features. This implies that a sound modeling of a catalyst poisoning process cannot leave out of consideration a detailed description of all the phenomena taking place within the catalyst itself, namely, reactant diffusion, main reaction and poisoning reaction.

As to the validity of the models proposed, these have shown good agreement with experimental data, thus affording some quantitative information to be collected concerning the poisoning kinetics of the reacting system considered, although an ultimate identification of the best-fitting model has not been possible. Therefore, further experimental study will be needed.

According to the experimental evidence, the models proposed in the present paper describe the catalyst deactivation patterns corresponding to a parallel poisoning mechanism

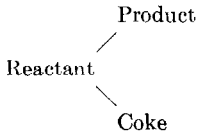

It is quite obvious that a completely different situation should be obtained for a series mechanism:

$$\text{Reactant} \rightarrow \text{Product} \rightarrow \text{Coke}$$

Acknowledgments

The assistance of Ing. Giorgio de Panno and Mr. Pietro Napolitano for both the theoretical and experimental parts of this work is gratefully acknowledged.

References

1. Prater, C. D., and Lago, R. M., *Advan. Catal.* **VIII**, 293 (1956).
2. Szepe, S., and Levenspiel, O., 4th European Symposium on Chemical Reaction Engineering, Brusells, 9–11 Sept. 1968.
3. Wheeler, A., *Advan. Catal.* **III**, 249 (1951).
4. Wheeler, A., Catalysis (P. H. Emmett, Ed.), vol. 2, Reinhold, New York, 1955.
5. Gioia, F., and Greco, G., Jr., *La Chim. l'Ind.*, **6**, 11 (1970).
6. Gioia, F., *I. & E. C. Fund.* **10**, 204 (1971).
7. Carberry, J. J., and Gorring, R. L., *J. Catal.* **5**, 529 (1966).
8. De Maldé, M., *La Chim. l'Ind.* **45**, 665 (1963).
9. De Maldé, M., Di Ció, G., Massi, and Mauri, M., *Hydrocarbon Process.* **43**, 164 (1964).
10. *Chem. Eng.* **28**, 78 (1964).
11. de Panno, G., Chemical Engineering Thesis, University of Naples, Naples, Italy, 1972.
12. Weekman, V. W., Jr., and Gorring, R. L., *J. Catal.* **4**, 260 (1965).
13. Satterfield, C. N., and Saraf, S. K., *I. & E. C. Fund.* **4**, 451 (1965).
14. Satterfield, C. N., and Cadle, P. J., *I. & E. C. Proc. Des. Dev.* **7**, 256 (1958).
15. Greco, G., Jr., *Ing. Chim. Ital.* **8**, 225 (1972).
16. Aris, R., *Chem. Eng. Sci.* **6**, 262 (1957).
17. Bischoff, K. B., *Chem. Eng. Sci.* **18**, 711 (1963).
18. Greensfelder, B. S., and Voge, H. H., *I. & E. C.* **1**, 514, (1945).
19. Hirschfelder, J. O., Curtiss, C. F., and Bird, R. B., "Molecular Theory of Gases and Liquids," Wiley, New York, 1954.
20. De Acetis, J., and Todos, G., *I. & E. C.* J. **52**, 1003 (1960).
21. Weisz, P. B., and Hicks, J. S., *Chem. Eng. Sci.* **17**, 265 (1962).
22. Hlaváček, V., Marék, M., *Collect. Czech. Chem. Commun.* **32**, 3291 (1967).

Nomenclature

a	available catalyst active area (cm^2/cm^3)
a^0	initial catalyst active area (cm^2/cm^3)
c	reactant concentration inside the pellet ($gmole/cm^3$)
c^0	reactant concentration in feed stream ($gmoles/cm^3$)
c_s	reactant concentration at the outer catalyst surface ($gmole/cm^3$)
D	effective reactant diffusion coefficient (cm^2/sec)
D_{12}	free diffusion coefficient (MBE in water vapor) (cm^2/sec)
D_K	Knudsen diffusion coefficient of MBE in the micropores (cm^2/sec)
E	activation energy of main reaction (gcal/gmoles)
h	heat transfer coefficient ($gcal/cm^2$ sec, °C)
k	kinetic constant of main reaction ($gmoles/cm^2$ sec)
k_c	mass transfer coefficient (cm/sec)
k_1	kinetic constant of coking reaction (zero order kinetics) (cm^2/cm^3 sec)
k_2	kinetic constant of coking reaction (1st order kinetics) ($cm^2/gmoles$ sec)

K	thermal conductivity of catalyst pellet (gcal/cm sec, °C)
N	reactant flux (gmoles/cm² sec)
q	heat flux (gcal/cm² sec)
Q	volumetric feed flow rate (liquid) (cm³/sec)
r	radial position (cm)
$\bar{r}_a$	mean macropore radius (Å)
$\bar{r}_i$	mean micropore radius (Å)
r^0	rate of main reaction, function of time (gmoles/cm³ sec)
R	pellet radius (cm)
t	time (sec)
T^0	bulk gas-phase temperature inside the reactor (°C)
T_s	outer catalyst surface temperature (°C)
x	conversion . . .
w	catalyst weight (g)
$\alpha = a/a^0$	dimensionless available area
$\beta = c_s(-\Delta H)D/T_sK$	maximum dimensionless temperature difference within the catalyst pellet
ϵ	total catalyst void fraction
ϵ_a	macropore void fraction
ϵ_i	micropore void fraction
$\gamma = c/c^0$	dimensionless reactant concentration
$\zeta = r/R$	dimensionless radial position
η	effectiveness factor
λ°	dimensionless reactant penetration at initial time
$\lambda(\tau)$, $\lambda(\tau')$	dimensionless reactant penetrations at τ and τ', respectively
ξ	ratio between present and initial reaction rates
$\pi(\tau)$, $\pi(\tau')$	dimensionless penetration of completely deactivated area, function of time τ and τ', respectively
$\rho(\tau)$	dimensionless overall rate of the main reaction, function of time
$\tau = k_1t/a^0$	dimensionless time
$\tau' = k_2c^0t/a^0$	dimensionless time
$\tau^*(\zeta)$	dimensionless time at which $\lambda(\tau)$ reaches a given radial position ζ
$\tau'^*(\zeta)$	dimensionless time at which $\pi(\tau')$ reaches a given radial position ζ
$\Phi = (ka^0R^2/c^0D)^{1/2}$	Thiele modulus